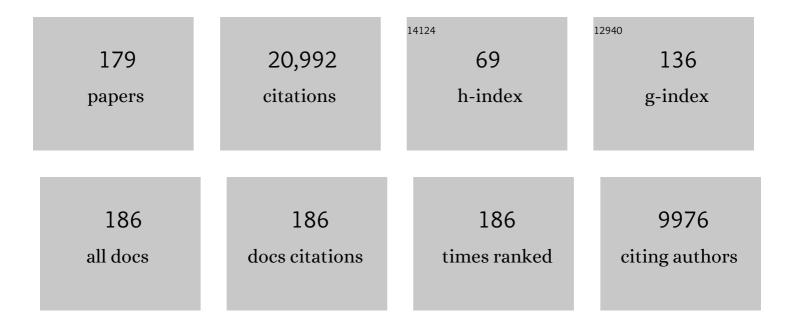
Mark D Zoback

List of Publications by Year in descending order

Source: https://exaly.com/author-pdf/6630976/publications.pdf Version: 2024-02-01



MADE D ZOBACE

#	Article	IF	CITATIONS
1	Long-term permeability evolution of shale seal rocks with argon and scCO2. Journal of Natural Gas Science and Engineering, 2022, 104, 104642.	2.1	2
2	Effects of Supercritical CO2 on Matrix Permeability of Unconventional Formations. Energies, 2021, 14, 1101.	1.6	8
3	Prior oil and gas production can limit the occurrence of injection-induced seismicity: A case study in the Delaware Basin of western Texas and southeastern New Mexico, USA. Geology, 2021, 49, 1198-1203.	2.0	15
4	A case study of vertical hydraulic fracture growth, stress variations with depth and shear stimulation in the Niobrara Shale and Codell Sand, Denver-Julesburg Basin, Colorado. Interpretation, 2021, 9, SG59-SG69.	0.5	5
5	Close Observation of Hydraulic Fracturing at EGS Collab Experiment 1: Fracture Trajectory, Microseismic Interpretations, and the Role of Natural Fractures. Journal of Geophysical Research: Solid Earth, 2021, 126, e2020JB020840.	1.4	28
6	Stability of the Fault Systems That Host-Induced Earthquakes in the Delaware Basin of West Texas and Southeast New Mexico. The Seismic Record, 2021, 1, 96-106.	1.3	23
7	Permeability Evolution of Fractures in Shale in the Presence of Supercritical CO ₂ . Journal of Geophysical Research: Solid Earth, 2021, 126, e2021JB022266.	1.4	6
8	Stratigraphically Controlled Stress Variations at the Hydraulic Fracture Test Site-1 in the Midland Basin, TX. Energies, 2021, 14, 8328.	1.6	4
9	Low Static Shear Modulus Along Foliation and Its Influence on the Elastic and Strength Anisotropy of Poorman Schist Rocks, Homestake Mine, South Dakota. Rock Mechanics and Rock Engineering, 2020, 53, 5257-5281.	2.6	7
10	Optimization of Multi-Stage Hydraulic Fracturing in Unconventional Reservoirs in the Context of Stress Variations with Depth. , 2020, , .		11
11	Predicting Lithology-Controlled Stress Variations in the Woodford Shale from Well Log Data via Viscoplastic Relaxation. SPE Journal, 2020, 25, 2534-2546.	1.7	13
12	A viscoplastic model of creep in shale. Geophysics, 2020, 85, MR155-MR166.	1.4	15
13	Multiscale variations of the crustal stress field throughout North America. Nature Communications, 2020, 11, 1951.	5.8	71
14	Production and Depletion. , 2019, , 345-374.		0
15	Stress, Pore Pressure, Fractures and Faults. , 2019, , 181-230.		0
16	Horizontal Drilling and Multi-Stage Hydraulic Fracturing. , 2019, , 233-262.		1
17	Composition, Fabric, Elastic Properties and Anisotropy. , 2019, , 31-64.		2

2

#	Article	IF	CITATIONS
19	Frictional Properties. , 2019, , 91-114.		0
20	Pore Networks and Pore Fluids. , 2019, , 115-148.		0
21	Flow and Sorption. , 2019, , 149-180.		0
22	Reservoir Seismology. , 2019, , 263-300.		0
23	Induced Shear Slip during Hydraulic Fracturing. , 2019, , 301-321.		0
24	Geomechanics and Stimulation Optimization. , 2019, , 322-344.		1
25	Environmental Impacts and Induced Seismicity. , 2019, , 377-405.		1
26	Managing the Risk of Injection-Induced Seismicity. , 2019, , 406-441.		0
27	The relation between stimulated shear fractures and production in the Barnett Shale: Implications for unconventional oil and gas reservoirs. Geophysics, 2019, 84, B461-B469.	1.4	34
28	Integrated Analysis of the Coupling Between Geomechanics and Operational Parameters to Optimize Hydraulic Fracture Propagation and Proppant Distribution. , 2019, , .		15
29	Injectionâ€Induced Seismicity and Faultâ€Slip Potential in the Fort Worth Basin, Texas. Bulletin of the Seismological Society of America, 2019, 109, 1615-1634.	1.1	52
30	Static and Dynamic Response of Bakken Cores to Cyclic Hydrostatic Loading. Rock Mechanics and Rock Engineering, 2018, 51, 1943-1953.	2.6	9
31	State of stress in the Permian Basin, Texas and New Mexico: Implications for induced seismicity. The Leading Edge, 2018, 37, 127-134.	0.4	89
32	Monitoring of cyclic steam stimulation by inversion of surface tilt measurements. The Leading Edge, 2018, 37, 350-355.	0.4	4
33	Microseismic evidence for horizontal hydraulic fractures in the Marcellus Shale, southeastern West Virginia. The Leading Edge, 2018, 37, 356-361.	0.4	30
34	Comparison of Short-Term and Long-Term Creep Experiments in Shales and Carbonates from Unconventional Gas Reservoirs. Rock Mechanics and Rock Engineering, 2018, 51, 1995-2014.	2.6	74
35	Fully Dynamic Spontaneous Rupture Due to Quasiâ€Static Pore Pressure and Poroelastic Effects: An Implicit Nonlinear Computational Model of Fluidâ€Induced Seismic Events. Journal of Geophysical Research: Solid Earth, 2018, 123, 9430-9468.	1.4	40
36	Physics-based forecasting of man-made earthquake hazards in Oklahoma and Kansas. Nature Communications, 2018, 9, 3946.	5.8	107

#	Article	IF	CITATIONS
37	Effects of Hydraulic Fracturing Fluid Chemistry on Shale Matrix Permeability. , 2018, , .		12
38	Imaging Pyrite Oxidation and Barite Precipitation in Gas and Oil Shales. , 2018, , .		15
39	The World Stress Map database release 2016: Crustal stress pattern across scales. Tectonophysics, 2018, 744, 484-498.	0.9	432
40	Predicted and observed shear on preexisting faults during hydraulic fracture stimulation. , 2018, , .		10
41	Lithology Variations and Cross-Cutting Faults Affect Hydraulic Fracturing of Woodford Shale: A Case Study. , 2017, , .		4
42	<i>In Situ</i> Stress and Active Faulting in Oklahoma. Bulletin of the Seismological Society of America, 2017, 107, 216-228.	1.1	106
43	The impacts of effective stress and CO2 sorption on the matrix permeability of shale reservoir rocks. Fuel, 2017, 203, 179-186.	3.4	45
44	Laboratory experiments simulating poroelastic stress changes associated with depletion and injection in lowâ€porosity sedimentary rocks. Journal of Geophysical Research: Solid Earth, 2017, 122, 2478-2503.	1.4	51
45	Lithology-controlled stress variations and pad-scale faults: A case study of hydraulic fracturing in the Woodford Shale, Oklahoma. Geophysics, 2017, 82, ID35-ID44.	1.4	46
46	Lithology-Controlled Stress Variations: A Case Study of the Woodford Shale, Oklahoma. , 2017, , .		0
47	Utilizing multiplets as an independent assessment of relative microseismic location uncertainty. The Leading Edge, 2017, 36, 829-836.	0.4	28
48	Response to Comment on "How will induced seismicity in Oklahoma respond to decreased saltwater injection rates?― Science Advances, 2017, 3, eaao2277.	4.7	28
49	Fully Coupled Nonlinear Fluid Flow and Poroelasticity in Arbitrarily Fractured Porous Media: A Hybridâ€Đimensional Computational Model. Journal of Geophysical Research: Solid Earth, 2017, 122, 7626-7658.	1.4	34
50	Permeability Evolution of Slowly Slipping Faults in Shale Reservoirs. Geophysical Research Letters, 2017, 44, 11,368.	1.5	79
51	Estimating geomechanical parameters from microseismic plane focal mechanisms recorded during multistage hydraulic fracturing. Geophysics, 2017, 82, KS1-KS11.	1.4	44
52	Utilizing A Viscoplastic Stress Relaxation Model to Study Vertical Hydraulic Fracture Propagation in Permian Basin. , 2017, , .		22
53	How will induced seismicity in Oklahoma respond to decreased saltwater injection rates?. Science Advances, 2016, 2, e1601542.	4.7	214
54	Experimental study of dynamic effective stress coefficient for ultrasonic velocities of Bakken cores. ,		4

2016, , .

#	Article	IF	CITATIONS
55	Effects of rock mineralogy and pore structure on stress-dependent permeability of shale samples. Philosophical Transactions Series A, Mathematical, Physical, and Engineering Sciences, 2016, 374, 20150428.	1.6	39
56	State of stress in Texas: Implications for induced seismicity. Geophysical Research Letters, 2016, 43, 10,208.	1.5	96
57	Probabilistic assessment of potential fault slip related to injection-induced earthquakes: Application to north-central Oklahoma, USA. Geology, 2016, 44, 991-994.	2.0	148
58	Viscoplastic Deformation of the Bakken and Adjacent Formations and Its Relation to Hydraulic Fracture Growth. Rock Mechanics and Rock Engineering, 2016, 49, 689-698.	2.6	57
59	Identification of Slowly Slipping Faults in the Barnett Shale Utilizing Ant-tracking. , 2015, , .		3
60	Fracture Gradient Prediction Using the Viscous Relaxation Model and Its Relation to Out-of-Zone Microseismicity. , 2015, , .		9
61	Characterizing and Responding to Seismic Risk Associated with Earthquakes Potentially Triggered by Fluid Disposal and Hydraulic Fracturing. Seismological Research Letters, 2015, 86, 1110-1118.	0.8	81
62	Joint estimation of acoustic properties, creep, and stress relaxation in organic-rich shales. , 2015, , .		0
63	Oklahoma's recent earthquakes and saltwater disposal. Science Advances, 2015, 1, e1500195.	4.7	350
64	Gas transport and storage capacity in shale gas reservoirs – A review. Part A: Transport processes. Journal of Unconventional Oil and Gas Resources, 2015, 12, 87-122.	3.5	204
65	To prevent earthquake triggering, pressure changes due to CO ₂ injection need to be limited. Proceedings of the National Academy of Sciences of the United States of America, 2015, 112, E4510.	3.3	27
66	Identification of fault-controlled damage zones in microseismic data – an example from the Haynesville shale. , 2015, , .		1
67	The role of preexisting fractures and faults during multistage hydraulic fracturing in the Bakken Formation. Interpretation, 2014, 2, SG25-SG39.	0.5	75
68	Utilizing Ant-tracking to Identify Slowly Slipping Faults in the Barnett Shale. , 2014, , .		6
69	Time-dependent subsidence associated with drainage-induced compaction in Gulf of Mexico shales bounding a severely depleted gas reservoir. AAPG Bulletin, 2014, 98, 1145-1159.	0.7	38
70	Predicting fault damage zones by modeling dynamic rupture propagation and comparison with field observations. Journal of Geophysical Research: Solid Earth, 2014, 119, 1251-1272.	1.4	54
71	Viscous relaxation model for predicting least principal stress magnitudes in sedimentary rocks. Journal of Petroleum Science and Engineering, 2014, 124, 416-431.	2.1	86
72	Experimental investigation of matrix permeability of gas shales. AAPG Bulletin, 2014, 98, 975-995.	0.7	394

#	Article	IF	CITATIONS
73	Adsorption of methane and carbon dioxide on gas shale and pure mineral samples. Journal of Unconventional Oil and Gas Resources, 2014, 8, 14-24.	3.5	587
74	A scaling law to characterize fault-damage zones at reservoir depths. AAPG Bulletin, 2014, 98, 2057-2079.	0.7	61
75	Time-dependent deformation of shale gas reservoir rocks and its long-term effect on the in situ state of stress. International Journal of Rock Mechanics and Minings Sciences, 2014, 69, 120-132.	2.6	252
76	The Effect of CO2 Adsorption on Permeability Anisotropy in the Eagle Ford Shale. , 2014, , .		40
77	Interpretation of unusual out-of-zone microseismicity in the Bakken Formation. , 2014, , .		1
78	Mechanical properties of shale-gas reservoir rocks — Part 2: Ductile creep, brittle strength, and their relation to the elastic modulus. Geophysics, 2013, 78, D393-D402.	1.4	286
79	Mechanical properties of shale-gas reservoir rocks — Part 1: Static and dynamic elastic properties and anisotropy. Geophysics, 2013, 78, D381-D392.	1.4	520
80	Experimental investigation of deformation mechanisms during shearâ€enhanced compaction in poorly lithified sandstone and sand. Journal of Geophysical Research: Solid Earth, 2013, 118, 4083-4100.	1.4	54
81	Long-period, long-duration seismic events during hydraulic stimulation of shale and tight-gas reservoirs — Part 1: Waveform characteristics. Geophysics, 2013, 78, KS97-KS108.	1.4	64
82	Frictional properties of shale reservoir rocks. Journal of Geophysical Research: Solid Earth, 2013, 118, 5109-5125.	1.4	193
83	Microseismicity and surface deformation of a heavy-oil reservoir undergoing cyclic steam stimulation. , 2013, , .		2
84	The Evolution of Stimulated Reservoir Volume during Hydraulic Stimulation of Shale Gas Formations. , 2013, , .		47
85	Long-period long-duration seismic events during hydraulic stimulation of shale and tight-gas reservoirs — Part 2: Location and mechanisms. Geophysics, 2013, 78, KS109-KS117.	1.4	27
86	Reply to Juanes et al.: Evidence that earthquake triggering could render long-term carbon storage unsuccessful in many regions. Proceedings of the National Academy of Sciences of the United States of America, 2012, 109, .	3.3	9
87	The Importance of Slow Slip on Faults During Hydraulic Fracturing Stimulation of Shale Gas Reservoirs. , 2012, , .		163
88	Stimulated Shale Volume Characterization: Multiwell Case Study from the Horn River Shale: I. Geomechanics and Microseismicity. , 2012, , .		34
89	Intraplate earthquakes, regional stress and fault mechanics in the Central and Eastern U.S. and Southeastern Canada. Tectonophysics, 2012, 581, 182-192.	0.9	74
90	Regional Stress Orientations and Slip Compatibility of Earthquake Focal Planes in the New Madrid Seismic Zone. Seismological Research Letters, 2012, 83, 672-679.	0.8	27

#	Article	IF	CITATIONS
91	Modeling evolution of the San Andreas Fault system in northern and central California. Geochemistry, Geophysics, Geosystems, 2012, 13, .	1.0	23
92	CO2 sequestration into the Wyodak coal seam of Powder River Basin—Preliminary reservoir characterization and simulation. International Journal of Greenhouse Gas Control, 2012, 9, 103-116.	2.3	16
93	Earthquake triggering and large-scale geologic storage of carbon dioxide. Proceedings of the National Academy of Sciences of the United States of America, 2012, 109, 10164-10168.	3.3	626
94	Hydraulic Fracturing, Microseismic Magnitudes, and Stress Evolution in the Barnett Shale, Texas, USA. , 2011, , .		128
95	Fracture characterization and fluid flow simulation with geomechanical constraints for a CO2–EOR and sequestration project Teapot Dome Oil Field, Wyoming, USA. Energy Procedia, 2011, 4, 3973-3980.	1.8	25
96	Long-period, long-duration seismic events during hydraulic fracture stimulation of a shale gas reservoir. The Leading Edge, 2011, 30, 778-786.	0.4	80
97	Viscous creep in room-dried unconsolidated Gulf of Mexico shale (II): Development of a viscoplasticity model. Journal of Petroleum Science and Engineering, 2010, 72, 50-55.	2.1	31
98	Climate and intraplate shocks. Nature, 2010, 466, 568-569.	13.7	5
99	Scientific Drilling Into the San Andreas Fault Zone. Eos, 2010, 91, 197-199.	0.1	124
100	Scaleâ€invariant stress orientations and seismicity rates near the San Andreas Fault. Geophysical Research Letters, 2010, 37, .	1.5	27
101	Oscillation of fluidâ€filled cracks triggered by degassing of CO ₂ due to leakage along wellbores. Journal of Geophysical Research, 2010, 115, .	3.3	17
102	Viscous creep in room-dried unconsolidated Gulf of Mexico shale (I): Experimental results. Journal of Petroleum Science and Engineering, 2009, 69, 239-246.	2.1	81
103	Constraining the far-field in situ stress state near a deep South African gold mine. International Journal of Rock Mechanics and Minings Sciences, 2009, 46, 555-567.	2.6	37
104	CO2 storage and enhanced coalbed methane recovery: Reservoir characterization and fluid flow simulations of the Big George coal, Powder River Basin, Wyoming, USA. International Journal of Greenhouse Gas Control, 2009, 3, 773-786.	2.3	59
105	Fluid Flow in a Fractured Reservoir Using a Geomechanically Constrained Fault-Zone-Damage Model for Reservoir Simulation. SPE Reservoir Evaluation and Engineering, 2009, 12, 562-575.	1.1	35
106	Seal integrity and feasibility of CO2 sequestration in the Teapot Dome EOR pilot: geomechanical site characterization. Environmental Geology, 2008, 54, 1667-1675.	1.2	143
107	Assessing the economic feasibility of regional deep saline aquifer CO2 injection and storage: A geomechanics-based workflow applied to the Rose Run sandstone in Eastern Ohio, USA. International Journal of Greenhouse Gas Control, 2008, 2, 230-247.	2.3	38
108	Hydraulic fracturing and wellbore completion of coalbed methane wells in the Powder River Basin, Wyoming: Implications for water and gas production. AAPG Bulletin, 2007, 91, 51-67.	0.7	76

#	Article	IF	CITATIONS
109	Did Earthquakes Keep the Early Crust Habitable?. Astrobiology, 2007, 7, 1023-1032.	1.5	34
110	The Role of Hydrocarbon Production on Land Subsidence and Fault Reactivation in the Louisiana Coastal Zone. Journal of Coastal Research, 2007, 233, 771-786.	0.1	83
111	Stress orientations of Taiwan Chelungpu-Fault Drilling Project (TCDP) hole-A as observed from geophysical logs. Geophysical Research Letters, 2007, 34, .	1.5	68
112	Predicting and monitoring long-term compaction in unconsolidated reservoir sands using a dual power law model. Geophysics, 2007, 72, E165-E173.	1.4	11
113	Assessing elastic Coulomb stress transfer models using seismicity rates in southern California and southwestern Japan. Journal of Geophysical Research, 2007, 112, .	3.3	45
114	Application of rate-and-state friction laws to creep compaction of unconsolidated sand under hydrostatic loading conditions. Journal of Geophysical Research, 2007, 112, .	3.3	4
115	Presentâ€day stress field in the Gibraltar Arc (western Mediterranean). Journal of Geophysical Research, 2007, 112, .	3.3	51
116	Stress, strain, and mountain building in central Japan. Journal of Geophysical Research, 2006, 111, n/a-n/a.	3.3	139
117	A multiscale study of the mechanisms controlling shear velocity anisotropy in the San Andreas Fault Observatory at Depth. Geophysics, 2006, 71, F131-F146.	1.4	123
118	Mapping stress and structurally controlled crustal shear velocity anisotropy in California. Geology, 2006, 34, 825.	2.0	146
119	Empirical relations between rock strength and physical properties in sedimentary rocks. Journal of Petroleum Science and Engineering, 2006, 51, 223-237.	2.1	700
120	Testing the use of aeromagnetic data for the determination of Curie depth in California. Geophysics, 2006, 71, L51-L59.	1.4	137
121	Impact of glacially induced stress changes on fault-seal integrity offshore Norway: Reply. AAPG Bulletin, 2005, 89, 275-279.	0.7	3
122	Viscous deformation of unconsolidated reservoir sands—Part 2: Linear viscoelastic models. Geophysics, 2004, 69, 742-751.	1.4	31
123	Viscous deformation of unconsolidated reservoir sands—Part 1: Timeâ€dependent deformation, frequency dispersion, and attenuation. Geophysics, 2004, 69, 731-741.	1.4	39
124	Regional tectonic stress near the San Andreas fault in central and southern California. Geophysical Research Letters, 2004, 31, .	1.5	212
125	Stress-induced seismic velocity anisotropy and physical properties in the SAFOD Pilot Hole in Parkfield, CA. Geophysical Research Letters, 2004, 31, .	1.5	124
126	A mechanical model of the San Andreas fault and SAFOD Pilot Hole stress measurements. Geophysical Research Letters, 2004, 31, .	1.5	48

#	Article	IF	CITATIONS
127	Stress orientations and magnitudes in the SAFOD pilot hole. Geophysical Research Letters, 2004, 31, .	1.5	214
128	Introduction to special section: Preparing for the San Andreas Fault Observatory at Depth. Geophysical Research Letters, 2004, 31, n/a-n/a.	1.5	104
129	Comprehensive wellbore stability analysis utilizing Quantitative Risk Assessment. Journal of Petroleum Science and Engineering, 2003, 38, 97-109.	2.1	149
130	Impact of glacially induced stress changes on fault-seal integrity offshore Norway. AAPG Bulletin, 2003, 87, 493-506.	0.7	25
131	Steady-State Failure Equilibrium and Deformation of Intraplate Lithosphere. International Geology Review, 2002, 44, 383-401.	1.1	155
132	Fault reactivation, leakage potential, and hydrocarbon column heights in the northern north sea. Norwegian Petroleum Society Special Publications, 2002, , 203-219.	0.1	30
133	Fault structure and kinematics of the Long Valley Caldera region, California, revealed by high-accuracy earthquake hypocenters and focal mechanism stress inversions. Journal of Geophysical Research, 2002, 107, ESE 9-1-ESE 9-19.	3.3	83
134	Production-induced Normal Faulting in the Valhall and Ekofisk Oil Fields. , 2002, , 403-420.		27
135	An integrated mechanical model of the San Andreas Fault in central and northern California. Journal of Geophysical Research, 2001, 106, 22051-22066.	3.3	75
136	Utilization of Mud Weights in Excess of the Least Principal Stress to Stabilize Wellbores: Theory and Practical Examples. SPE Drilling and Completion, 2001, 16, 221-229.	0.9	29
137	Implications of hydrostatic pore pressures and high crustal strength for the deformation of intraplate lithosphere. Tectonophysics, 2001, 336, 19-30.	0.9	350
138	Implications of earthquake focal mechanisms for the frictional strength of the San Andreas fault system. Geological Society Special Publication, 2001, 186, 13-21.	0.8	62
139	Did deglaciation trigger intraplate seismicity in the New Madrid seismic zone?. Geology, 2001, 29, 175.	2.0	103
140	Strength of the San Andreas. Nature, 2000, 405, 31-32.	13.7	88
141	How faulting keeps the crust strong. Geology, 2000, 28, 399.	2.0	782
142	Fracture permeability and in situ stress to 7 km depth in the KTB scientific drillhole. Geophysical Research Letters, 2000, 27, 1045-1048.	1.5	138
143	How faulting keeps the crust strong. Geology, 2000, 28, 399-402.	2.0	62
144	Seismic Hazard at the New Madrid Seismic Zone. Science, 1999, 285, 663d-663.	6.0	3

#	Article	IF	CITATIONS
145	Lithospheric strength and intraplate seismicity in the New Madrid seismic zone. Tectonics, 1997, 16, 585-595.	1.3	156
146	Estimation of the complete stress tensor to 8 km depth in the KTB scientific drill holes: Implications for crustal strength. Journal of Geophysical Research, 1997, 102, 18453-18475.	3.3	401
147	Anelasticity and dispersion in dry unconsolidated sands. International Journal of Rock Mechanics and Minings Sciences, 1997, 34, 48.e1-48.e12.	2.6	15
148	The San Andreas Fault Zone Drilling Project: Scientific Objectives and Technological Challenges. Journal of Energy Resources Technology, Transactions of the ASME, 1995, 117, 263-270.	1.4	4
149	Fluid flow along potentially active faults in crystalline rock. Geology, 1995, 23, 683.	2.0	745
150	Compressive and tensile failure of inclined well bores and determination of in situ stress and rock strength. Journal of Geophysical Research, 1995, 100, 12791-12811.	3.3	255
151	TOWARDS ESTABLISHMENT OF AN INTERNATIONAL CONTINENTAL SCIENTIFIC DRILLING PROGRAM. Terra Nova, 1994, 6, 3-4.	0.9	5
152	Stress perturbations associated with active faults penetrated by boreholes: Possible evidence for near-complete stress drop and a new technique for stress magnitude measurement. Journal of Geophysical Research, 1994, 99, 9373-9390.	3.3	189
153	Deep scientific drilling in the San Andreas Fault Zone. Eos, 1994, 75, 137.	0.1	21
154	Upper-crustal strength inferred from stress measurements to 6 km depth in the KTB borehole. Nature, 1993, 365, 633-635.	13.7	159
155	Mechanism Diversity of the Loma Prieta Aftershocks and the Mechanics of Mainshock-Aftershock Interaction. Science, 1993, 259, 210-213.	6.0	122
156	State of stress in the Long Valley caldera, California. Geology, 1993, 21, 837.	2.0	43
157	Transform-normal extension and asymmetric basins: An alternative to pull-apart models. Geology, 1992, 20, 423.	2.0	134
158	Selfâ€similar distribution and properties of macroscopic fractures at depth in crystalline rock in the Cajon Pass Scientific Drill Hole. Journal of Geophysical Research, 1992, 97, 5181-5200.	3.3	187
159	In situ stress measurements to 3.5 km depth in the Cajon Pass Scientific Research Borehole: Implications for the mechanics of crustal faulting. Journal of Geophysical Research, 1992, 97, 5039-5057.	3.3	329
160	Stress orientation profile to 3.5 km depth near the San Andreas Fault at Cajon Pass, California. Journal of Geophysical Research, 1992, 97, 5059-5080.	3.3	146
161	Utilization of observations of well bore failure to constrain the orientation and magnitude of crustal stresses: Application to continental, Deep Sea Drilling Project, and Ocean Drilling Program boreholes. Journal of Geophysical Research, 1990, 95, 9305-9325.	3.3	360
162	Chapter 24: Tectonic stress field of the continental United States. Memoir of the Geological Society of America, 1989, , 523-540.	0.5	204

#	Article	IF	CITATIONS
163	Global patterns of tectonic stress. Nature, 1989, 341, 291-298.	13.7	571
164	Empirical relationships among seismic velocity, effective pressure, porosity, and clay content in sandstone. Geophysics, 1989, 54, 82-89.	1.4	404
165	Inâ€situ stress orientation and magnitude at the Fenton Geothermal Site, New Mexico, determined from wellbore breakouts. Geophysical Research Letters, 1988, 15, 467-470.	1.5	212
166	The Cajon Pass Scientific Drilling Experiment: Overview of phase 1. Geophysical Research Letters, 1988, 15, 933-936.	1.5	37
167	In situ stress orientation near the San Andreas Fault: Preliminary results to 2.1 km depth from the Cajon Pass Scientific Drillhole. Geophysical Research Letters, 1988, 15, 989-992.	1.5	25
168	Hydraulic fracturing in situ stress measurements to 2.1 km depth at Cajon Pass, California. Geophysical Research Letters, 1988, 15, 1005-1008.	1.5	31
169	<i>In situ</i> permeability and fluid pressure measurements at â^1⁄42 km depth in the Cajon Pass research well. Geophysical Research Letters, 1988, 15, 1029-1032.	1.5	48
170	New Evidence on the State of Stress of the San Andreas Fault System. Science, 1987, 238, 1105-1111.	6.0	896
171	In situ stress, natural fracture distribution, and borehole elongation in the Auburn Geothermal Well, Auburn, New York. Journal of Geophysical Research, 1985, 90, 5497-5512.	3.3	93
172	Well bore breakouts and in situ stress. Journal of Geophysical Research, 1985, 90, 5523-5530.	3.3	644
173	State of Stress and Intraplate Earthquakes in the United States. Science, 1981, 213, 96-104.	6.0	103
174	Recurrent Intraplate Tectonism in the New Madrid Seismic Zone. Science, 1980, 209, 971-976.	6.0	87
175	State of stress in the conterminous United States. Journal of Geophysical Research, 1980, 85, 6113-6156.	3.3	735
176	The effect of microcrack dilatancy on the permeability of westerly granite. Journal of Geophysical Research, 1975, 80, 752-755.	3.3	352
177	The effect of cyclic differential stress on dilatancy in westerly granite under uniaxial and triaxial conditions. Journal of Geophysical Research, 1975, 80, 1526-1530.	3.3	137
178	Tectonic stress field of North America and relative plate motions. , 0, , 339-366.		78
179	Predicting variations of the least principal stress with depth: Application to unconventional oil and gas reservoirs using a log-based viscoelastic stress relaxation model. Geophysics, 0, , 1-56.	1.4	1